FIRST EVIDENCE OF $WW/WZ \to \ell\nu q\bar{q}$ AT THE TEVATRON

JOSEPH HALEY

(For the D0 Collaboration)

Princeton University Department of Physics

Princeton, NJ, USA

We present the first evidence from a hadron collider of $WW + WZ$ production with semi-leptonic decays. The data were recorded by the D0 detector at the Fermilab Tevatron and correspond to 1.07 fb^{-1} of integrated luminosity obtained in proton-antiproton collisions at $\sqrt{s} =$ 1.96 TeV. The cross section observed for $WW + WZ$ production is 20.2 ± 4.5 pb with a significance of 4.4 standard deviations.

1 Introduction

There are many reasons for studying $WW/WZ \to \ell\nu q\bar{q}$ at the Tevatron. From the electroweak prospective, diboson production provides a probe of self-interactions of vector bosons. Deviations from the Standard Model (SM) of these trilinear gauge boson coupling would affect the cross sections and event kinematics of diboson production[1]. The cross sections for diboson production at the Tevatron had previously only been measured for the fully leptonic final states[2,3], so this analysis provides a compliment to the previous measurements.

Reconstruction of WW and WZ events in semi-leptonic final states represents a challenge in separating signal from the dominant background of a W boson produced in association with jets. This is a challenge shared by many Higgs boson searches, *e.g.* $WH \to \ell\nu b\bar{b}$, making this measurement a benchmark for these similar Higgs boson searches. Furthermore, this analysis provides a proving ground for the multivariate event-classification schemes and the accompanying statistical techniques[4] that are used for the Tevatron Higgs boson searches in the entire mass range allowed by the SM.

2 Event Selection

To select candidate events for $p\bar{p} \to WW/WZ \to \ell\nu q\bar{q}$, we required a single reconstructed lepton (electron or muon)[6] with transverse momentum $p_T > 20$ GeV and $|\eta| < 1.1$ (for electrons) or

$|\eta| < 2$ (for muons), an imbalance in transverse momentum $\not{E}_T > 20$ GeV, and at least two jets[7] with $p_T > 20$ GeV and $|\eta| < 2.5$. The leading jet (*i.e.* highest p_T) was also required to have $p_T > 30$ GeV. To reduce background from processes that do not contain $W \to \ell\nu$, we required a transverse W mass of $M_T^W > 35$ GeV, where $M_T \equiv \sqrt{(E_T)^2 - (\vec{p}_T)^2}$[8]. The electron or muon trajectories were required to be isolated from other objects in the calorimeter, and had to match a track reconstructed in the central tracking system that originated from the primary vertex. Also, the muon had to be reconstructed as an isolated track in the central tracking system.

3   Event Samples

The data were collected with the D0 detector[5] at the Fermilab Tevatron Collider at a center-of-mass energy of $\sqrt{s} = 1.96$ TeV. The events studied in this analysis correspond to 1.07 fb^{-1} of integrated luminosity collected during Run IIa (2002-2006). To be considered for analysis, events in the $e\nu q\bar{q}$ channel were required to pass at least one single electron or electron+jet(s) trigger. The resulting trigger efficiency was $98^{+2}_{-3}\%$. A suite of triggers was used for the $\mu\nu q\bar{q}$ channel resulting in a trigger efficiency of nearly 100%.

Monte Carlo generators were used to simulate the signal and background samples that contained a charged lepton in the final state. With the exception of W+jets, all background MC samples were normalized to next-to-leading-order (NLO) or next-to-next-to-leading-order SM predictions. The W+jets normalization was determined simultaneously with the signal cross section by a fit to data, as discussed later.

The background from multijet events was estimated using an orthogonal selection of data in each channel. In both case, the contribution from events that were already modeling via MC was corrected for.

4   Multivariate Classification

Improved separation between the signal and the backgrounds was achieved using a multivariate classification technique to combine information from several kinematic variables. The technique used was a random forest (RF) classifier[15,16] from the STATPATTERNRECOGNITION[16] software package. The RF algorithm creates many decision tree classifiers, which are basically a series of optimized binary splits to separate signal from background. The RF is then formed by taking the average of all of the decision trees. The key to the RF is that each decision tree uses only a subset of the input variables (selected randomly for each tree) and is trained on a bootstrap replica[15] of the full training set. This results in each of the trees generalizing differently to unseen data because each tree was trained with differently. The net effect of then averaging all the trees is an accurate and stable classifier.

The inputs to the RF were thirteen well-modeled kinematic variables that demonstrated a difference in probability density between signal and at least one of the backgrounds. A RF for each channel was trained using one half of each MC sample. The other halves, along with the multijet background samples, were used to evaluate the RF output distributions for comparison to the data. These RF output distributions were then used to measure the excess of events in the data consistent with the kinematics of WW and WZ production (over that expected from multijet and other SM processes).

5   Cross Section Measurement

The cross section for $WW + WZ$ production was determined from a fit of signal and background RF templates to the data by minimizing a Poisson χ^2 function within variations of the systematic uncertainties[4]. The systematic uncertainties were treated as Gaussian-distributed uncertainties

on the expected numbers of signal and background events in each bin of the RF distribution. Each individual uncertainty was treated as 100% correlated between channels, samples, and from bin to bin. Different sources of uncertainty were assumed to be independent.

The normalizations of the RF templates for the signal and the W+jets background were unconstrained in the fit; allowing the fit to simultaneously measured the signal cross section and determine the normalization of the dominant background. This approach eliminated the need to use the W+jets cross section predicted by ALPGEN and provided an unbiased uncertainty for the normalization of the dominant background. As a check of the procedure, the fit yielded an effective k-factor of 1.53 ± 0.13 that needed to be applied to the ALPGEN cross section to best match the data, which is close to what one would expected from the ratio of NLO to LO predictions for the W+jets cross section.

Table 1 contains the results of the fit in the $e\nu q\bar{q}$, $\mu\nu q\bar{q}$, and the combined channels. The RF output distribution after the combined fit and the same plot with the background subtracted are shown in Fig. 1. Also in Fig. 1 is the background-subtracted plot for the dijet mass distribution showing the resonant dijet signal peak observed in data. The common behavior of each fit indicates a $WW + WZ$ cross section consistent with, though somewhat larger than, the expected SM value of $\sigma(WW + WZ) = 16.1$ pb[17]. The combined lepton channel cross section fit yielded a total value of $20.2 \pm 2.5(\text{stat}) \pm 3.6(\text{sys}) \pm 1.2(\text{lum})$ pb, which is slightly less that one standard deviation from expectation.

Table 1 also provides the result from preforming the measurement using only the dijet mass distribution. As expected, the measurement from the dijet mass distribution was less precise than from the RF because the RF was better at discriminating signal from background.
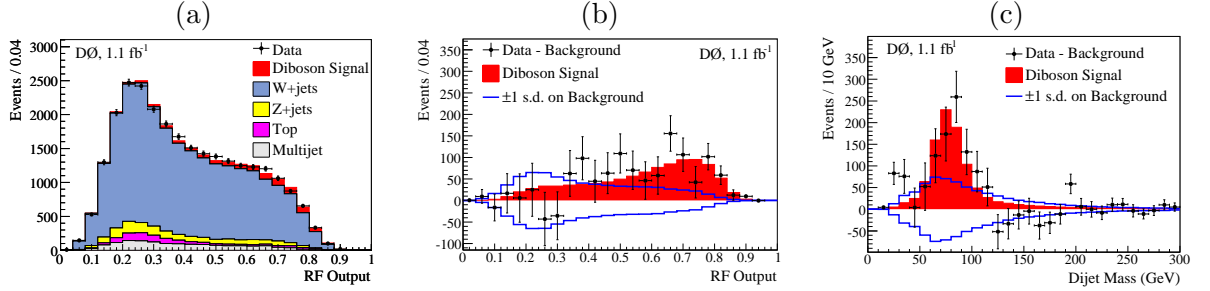

Figure 1: The distributions after cross section fit of the RF distribution: (a) RF output; (b) RF output with background subtracted; (c) dijet mass with background subtracted.

Table 1: The signal cross section determined from a simultaneous fit to the data of the $WW + WZ$ cross section and the normalization factor for W+jets.

Channel	Fitted signal σ (pb)
$e\nu q\bar{q}$ RF Output	$18.0\pm3.7(\text{stat})\pm5.2(\text{sys})\pm1.1(\text{lum})$
$\mu\nu q\bar{q}$ RF Output	$22.8\pm3.3(\text{stat})\pm4.9(\text{sys})\pm1.4(\text{lum})$
Combined RF Output	$20.2\pm2.5(\text{stat})\pm3.6(\text{sys})\pm1.2(\text{lum})$
Combined Dijet Mass	$18.5\pm2.8(\text{stat})\pm4.9(\text{sys})\pm1.1(\text{lum})$

6 Significance

Arguably just as important as the cross sections measurement is the significance of the measurement. The expected and observed significances were obtained via fits of the signal plus background hypothesis to MC events drawn from the background-only hypothesis[18]. The pseudo-data samples were generated from random Poisson trials seeded by the predicted number of

background events smeared within the systematic uncertainties. A measurement of the signal cross section was performed on each of the background-only pseudo-data distributions just as for the data. The *expected* significance corresponds to the fraction of outcomes that yielded a cross section at least as large as the SM prediction for $WW + WZ$ production. The *observed* significance was determined by the fraction of outcomes above the measured cross section.

Table 2 gives the probability (p-value) and Gaussian significance (number of standard deviations for the corresponding Gaussian confidence level) for expected and observed outcomes corresponding to the measurements in Table 1. Again one can see the merit of the multivariate classifier. While the observed significance using the dijet mass was found to be 3.3 standard deviation, the RF had an observed significance of 4.4 standard deviations.

Table 2: Expected and observed p-values obtained by comparing the measurement with background-only pseudo-experiments and the corresponding significance in number of standard deviations (s.d.) for a one-sided Gaussian integral.

Channel	Expected p-value (significance)	Observed p-value (significance)
$e\nu q\bar{q}$ RF Output	6.8×10^{-3} (2.5 s.d.)	3.2×10^{-3} (2.7 s.d.)
$\mu\nu q\bar{q}$ RF Output	1.8×10^{-3} (2.9 s.d.)	5.2×10^{-5} (3.9 s.d.)
Combined RF Output	1.5×10^{-4} (3.6 s.d.)	5.4×10^{-6} (4.4 s.d.)
Combined Dijet Mass	1.7×10^{-3} (2.9 s.d.)	4.4×10^{-4} (3.3 s.d.)

7 Conclusions

Using semi-leptonic decay channels, we measured $\sigma(WW + WZ) = 20.2 \pm 4.5$ pb in proton-antiproton collisions $\sqrt{s} = 1.96$ TeV. This is consistent with the SM prediction of $\sigma(WW + WZ) = 16.1 \pm 0.9$ pb as well as with previous measurements of WW and WZ in the fully leptonic final states [2,3]. The significance of the measurement is 4.4 standard deviations about the background, indicating the first direct evidence for $WW+WZ$ production with semi-leptonic decays at a hadron collider. Finally, this analysis demonstrates the ability to measure a small signal in a large background for a final state of direct relevance to searches for a low mass Higgs boson and provides a validation of the analytical methods used in searches for Higgs bosons at the Tevatron [19].

References

1. K. Hagiwara, S. Ishihara, R. Szalapski and D. Zeppenfeld, Phys. Rev. D **48** (1993).
2. D0 Collaboration: V. M. Abazov *et al.*, Phys. Rev. Lett. **94**, 151801 (2005); Phys. Rev. D **76**, 111104(R) (2007); Phys. Rev. Lett. **101**, 171803 (2008).

3. CDF Collaboration: D. Acosta *et al.*, Phys. Rev. Lett. **94**, 211801 (2005); A. Abulencia *et al.*, Phys. Rev. Lett. **98**, 161801 (2007); T. Aaltonen *et al.*, Phys. Rev. Lett. **100**, 201801 (2008).

4. W. Fisher, FERMILAB-TM-2386-E (2006).

5. B. Abbott *et al.* (D0 Collaboration), Nucl. Instrum. Methods Phys. Res. A **565**, 463 (2006).

6. V. M. Abazov *et al.* (D0 Collaboration), Phys. Lett. B **626**, 45 (2005).

7. G. C. Blazey *et al.*, arXiv:hep-ex/0005012 (2000). The seeded cone algorithm with radius 0.5 was used.

8. J. Smith, W. L. van Neerven, and J. A. M. Vermaseren, Phys. Rev. Lett. **50**, 1738 (1983).

9. T. Sjöstrand *et al.*, Comput. Phys. Commun. **135**, 238 (2001). Verison 6.3 was used.

10. M. L. Mangano *et al.*, JHEP **0307**, 001 (2003). Version 2.05 was used.

11. A. Pukhov *et al.*, arXiv:hep-ph/9908288 (2000).

12. R. Brun, F. Carminati, CERN Program Library Long Writeup W5013 (1993).

13. J. Alwall *et al.*, Eur. Phys. C **53**, 473 (2008).

14. S. Höche *et al.*, arXiv:hep-ph/0602031 (2006).

15. L. Breiman, Machine Learning **45**, 5 (2001).

16. I. Narsky, arXiv:physics/0507143 [physics.data-an] (2005).

17. J. M. Campbell and R. K. Ellis, Phys. Rev. D **60**, 113006 (1999). Cross sections were calculated with the same parameter values given in the paper, except with $\sqrt{s} = 1.96$ TeV.

18. V. M. Abazov *et al.* (D0 Collaboration), Phys. Rev. D **78**, 012005 (2008).

19. TEVNPH Working Group, for the CDF Collaboration and D0 Collaboration, arXiv:0804.3423 [hep-ex] (2008).